JOURNAL OF APPLIED ELECTROCHEMISTRY **28** (1998) 689–696

Electrochemical reduction of nickel ions from dilute artificial solutions in a GBC reactor

K. N. NJAU, Y. M. HOSSEINI and L. J. J. JANSSEN

Eindhoven University of Technology, Department of Chemical Engineering, Laboratory of Instrumental Analysis, PO Box 513, 5600 MB Eindhoven, The Netherlands

Received 19 June 1996; revised 2 December 1997

The electrochemical reduction of nickel ions from a dilute solution has been carried out in a 'gas diffusion electrode packed bed electrode cell' (GBC). Particle size and electrode configuration have been found to have a significant influence on the reduction process. Electrodes with a high porosity and large pores have been found to be the best for nickel deposition. The nickel current efficiency, η_{Ni}, is reported to be dependent on the current density, volumetric flow rate, nickel and boric acid concentration, and the pH. The fall in the nickel current efficiency is caused by an increase in electrode surface pH above a certain level, caused by either high bulk solution pH or high current density, leading to possibly formation of $Ni(OH)_2$. It has been found that under conditions of exclusively metallic nickel deposition $\eta_{Ni}/(1-\eta_{Ni})$ is proportional to $i^{0.69}, Q_1^{0.52}, C_{Ni}^{0.67}, C_{BA}^{-0.19}$ and $pH^{1.0}$.

Keywords: *nickel deposition*, *gas diffusion electrode*, *packed bed*

1. Introduction

Aqueous liquors containing low levels of nickel ions (less than $1\,g\,dm^{-3}$) are routinely generated during nickel electroplating. Traditionally, these solutions have been treated by chemical precipitation, using a cheap reagent such as lime or caustic soda. Following sedimentation, the insoluble hydroxide sludge is separated by filtration. Sludge disposal is becoming an increasing problem due to restrictions on transport and ever more limited facilities for bore hole, sea or land fill dumping. Sludge formation entails both a return to a combined state, for example metal hydroxides, oxides and other compounds, and a waste of material and energy.

Today some electroplating plants use ion exchangers (IOX) to treat low metal concentration rinse waters. This is particularly true for a nickel line, the rinse water of which offers a good pH range for optimum use of ion exchangers. The IOX method, however also has some limitations, such as the disposal of wastes resulting from spent regenerant chemicals, and limitation to the maximum concentration of metal ions to be treated. Moreover, metals cannot be directly recovered in their metallic form [1].

In many plating operations, the nickel salt recovered from the ion exchange can be recycled back into the plating bath. However, there is a reluctance to recycle chemicals in many operations because of the high value of the product and the perceived risk in using reclaimed material. In such cases, electrowinning of nickel may be the preferred route.

Electrochemical recovery of nickel from rinse water is of interest, due to the fact that pure metal may be recovered without the necessity of disposal of nickel containing sludge or regeneration of nickel loaded saturated ion exchanger resin. In practice, the type of cathode in the electrochemical cell for the recovery of metals from dilute solutions depends on the range of metal ion concentration. Two ranges of metal ion concentration are considered [2]:

(i) Metal ion concentration $> 1\,g\,dm^{-3}$ of solution, for which two dimensional cathodes are used to obtain concentration levels in the range 0.1 to $0.5\,g\,dm^{-3}$.
(ii) Metal ion concentrations up to $0.1\,g\,dm^{-3}$, for which a three-dimensional electrode is preferred.

Different forms of cathode have been applied in the recovery of metal ions electrochemically, either as two dimensional electrodes or three dimensional electrodes. The two dimensional electrodes have mostly taken the form of a simple vertical metal plate, a metal gauze or expanded metal sheets, placed into a rotating electrode cell or tank units where turbulence is promoted by using an inert fluidized bed. The three-dimensional electrode is either a fluidized bed, a fixed bed or a porous electrode [2]. Three dimensional electrodes can be constructed with carbon and metal particles, graphite/carbon felts, expanded metal sheets and reticulated vitreous carbon (RVC) and other metal form-like materials. The RVC has a honeycomb structure, with open pores and has a high surface to volume ratio. It is available in different grades of porosity and pore size ranging from 70–97% and 10 to 100 ppi (pores per inch), respectively [3, 4].

The GBC (gas diffusion electrode packed bed electrode cell) process discussed in [5–8] provides an alternative, cleaner technology which utilizes hydrogen gas to reduce metal ions. The use of GBC for the

0021-891X

reduction of nickel ions demands the operation of the reactor in a divided mode because the Gibbs free energy of the nickel ion reduction by hydrogen is positive, thus requiring an external source of energy. The use of a hydrogen gas diffusion anode in the GBC reactor makes single liquid circuit operation possible without generation of gases on the anode.

The advantages of using a GBC reactor for nickel reduction are as follows:

(i) lower cell voltages compared to the use of oxygen or chlorine evolving anodes;
(ii) chloride based systems may be treated in single liquid circuit cell without generation of toxic chlorine gas;
(iii) higher current efficiency for nickel deposition since no oxygen or chlorine is introduced by the anode reaction; and
(iv) no formation of chlorinated organic compounds.

The reduction of nickel ions in synthetic made solutions was investigated earlier, using a rotating disc electrode [7]. In this work, further investigation using a GBC reactor is carried out to select the optimal conditions of electrolysis for nickel recovery in the GBC reactor. The effects of electrolysis current, nickel ion concentration, boric acid concentration and temperature on current efficiency for nickel deposition are determined. The effect of cathode configuration is reported.

2. Experimental details

2.1. *The set-up*

The experimental set-up was a batch recycle system consisting of a laboratory-scale cell, a 3 dm^3 solution storage vessel, a pump, a flow meter and a heat exchanger. A schematic representation of the set-up is shown in Fig. 1.

A schematic representation of the cell is shown in Fig. 2. The cathode chamber had a thickness of 0.8 cm, a height of 2.5 cm and width of 2.5 cm and was completely filled with the porous cathode. A graphite plate of about 5 mm thick placed at the back of the cathodic cell compartment was used as a current feeder to the three dimensional electrode.

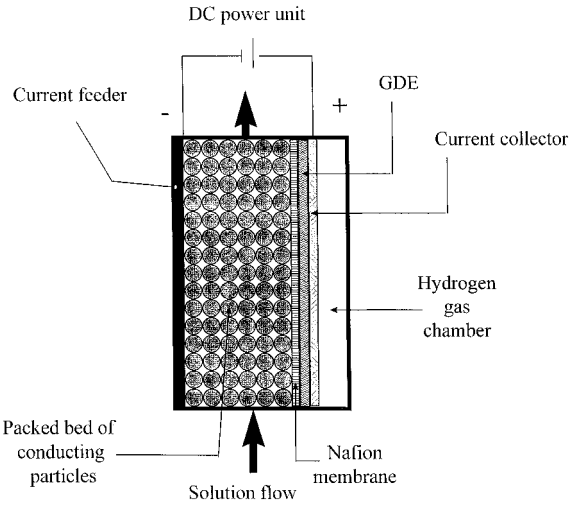

Fig. 2. Schematic representation of GBC cell.

Three types of materials were used for the cathode. The first consisted of a bed of graphite particles of various sizes between 1–6 mm and of irregular shape. The second was reticulated vitreous carbon (RVC) from ElectroCell AB. Two types of RVC were used, namely RVC-10, which had a porosity of 0.97 and was 10 ppi (pores per inch), and RVC-100, with a porosity of 0.91 and 100 ppi. The third was a stack of expanded nickel sheets.

A silver wire reference electrode was inserted at the entrance of the cell along the cathode width, without touching the cathode.

The anode was a fuel cell grade gas diffusion electrode (GDE) with a geometric surface area of 6.25 cm^2 (2.5 cm × 2.5 cm). Two types of gas diffusion electrode were used, namely a fuel Cell Grade on Toray, paper purchased from E-TEK, USA,

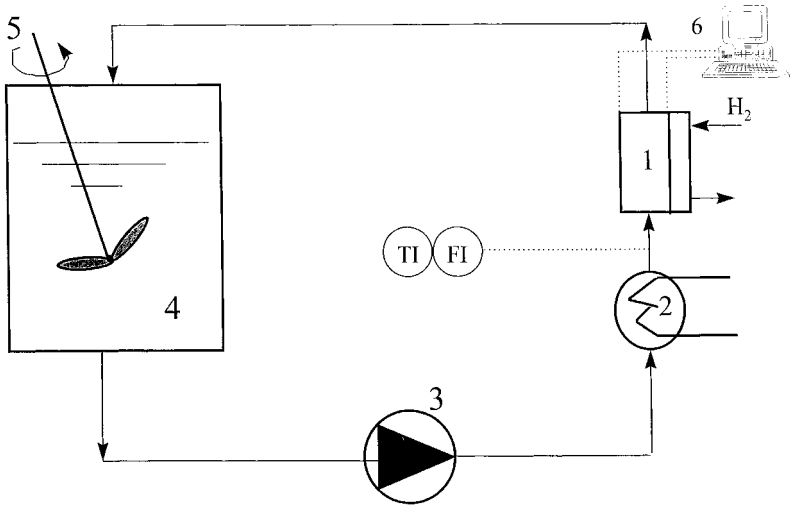

Fig. 1. Scheme of the experimental set-up: (1) GBC-cell (2) heat exchanger (3) a solution pump (4) glass vessel (5) mechanical stirrer (6) to data acquisition system.

called E-TEK-GDE, and an E-TEK Elat vulcan electrode covered by a Nafion®-117 layer on one side, called ECN–GDE. The E-TEK-GDE had a platinum loading of $0.50\,mg\,cm^{-2}$, while the ECN–GDE had $0.4\,mg\,cm^{-2}$. The gas diffusion electrode was supported by a perforated platinum plate placed on the gas side as a current collector and to enhance mechanical stability. When the E-TEK-GDE was used, it was necessary to provide an electrical insulation between the packed bed cathode and the anode. This was achieved either by the use of a Nafion®-117 membrane or a perforated Perspex plate of thickness 4 mm with holes of 2 mm diameter. Both were placed on the liquid side of the GDE. The ECN–GDE did not require an extra separator because of the Nafion®117 membrane already pressed on the electrode.

2.2. *Solutions and analysis*

Laboratory solutions of nickel sulfate (Merck, p.a), boric acid (Merck, extra pure) and sodium sulfate (Merck, extra pure) of various concentrations were used. Millipore water was used to make the solutions. Unless otherwise stated, the standard conditions listed in Table 1 were used. Before each run, nitrogen gas was purged through the solution in the vessel and through the gas compartment of the cell to prevent the reaction of hydrogen with oxygen inside the GDE. During the electrolysis, the gas diffusion electrode was fed with pure hydrogen from a gas cylinder and nitrogen gas was purged through the solution in the glass vessel. The pH of the solution was maintained constant throughout an electrolysis run by additions of 1 M NaOH solution and was controlled by a combination of a digital pH meter type PHM 63 and a titrator type TTT80 from Radiometer A/S Copenhagen.

The determination of the nickel ion concentration was done using an Atomic Absorption Spectrophotometer (AAS) (Perkin–Elmer 3030). Deposition experiments were carried out galvanostatically, using either a computer controlled, digital potentiostat (Autolab PGSTAT20, Eco-Chemie) or a d.c.-current generator (Delta Electronika Power supply E-030-1).

Table 1. Standard conditions of the experiments

Parameter	*Value*
Bath composition	
Starting nickel concentration	$5\,mol\,m^{-3}$
Boric acid concentration	$0.1\,kmol\,m^{-3}$
Sodium sulfate concentration	$0.1\,kmol\,m^{-3}$
Ammonium Sulfate	$20\,mol\,m^{-3}$
Electrolysis conditions	
Flow rate of solution	$21\,cm^3\,s^{-1}$
Temperature	298 K
pH of bulk solution	5
Deposition time	1 h
Current density	$320\,A\,m^{-2}$
Volume of solution	$1\,dm^3$
Electrode parameters	
Cathode	Bed of graphite particles
Size	$2\,mm < d < 4\,mm$
Geometric surface area of cathode	$6.25\,cm^2$
Anode	ECN–GDE
Geometric surface area of anode	$6.25\,cm^2$

3. Results

3.1. *Potential–current density and potential–time curves*

The bed of graphite particles was polarized at a potential scan rate of $5\,mV\,s^{-1}$ from −0.4 to −1.3 V and back under standard conditions. Current densities were calculated based on the GDE geometric surface. The results of the relationship between the current density and cathode potential are shown in Fig. 3. No ohmic correction was applied. The scan in the cathodic potential direction shows a very weak reduction wave between about −0.5 to −0.85 V. With increased cathodic potential, the curve shows a rapid increase in the current density, probably due to higher rates of hydrogen evolution.

In another experiment, the cathode potential was measured as a function of electrolysis time during nickel deposition on RVC-100 at two current densities, namely 320 and $800\,A\,m^{-2}$ under standard conditions. The results are shown in Fig. 4. From Fig. 4, it can be inferred that, at the highest current density, blockage of the electrode by hydrogen gas bubbles occurred. In these experiments, it was observed that only a layer of about 0.75 mm and 2 mm of the RVC-100, next to the GDE, was covered with nickel for 320 and $800\,A\,m^{-2}$, respectively. Moreover the layer of RVC-100 covered with nickel deposit was clearly thicker at the solution outlet than at the inlet (by about a factor of 2).

3.2. *Decrease of nickel concentration during electrolysis*

An experiment was conducted for a long duration, using a solution with the standard composition but without boric acid. The electrode parameters and electrolysis conditions were retained, as in Table 1. A

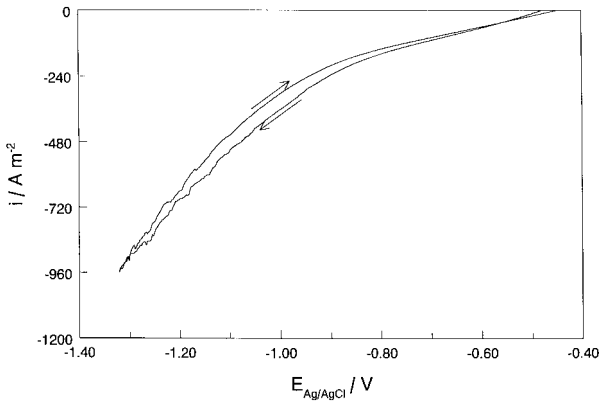

Fig. 3. Plot of potential of the packed bed electrode against the current density at standard conditions.

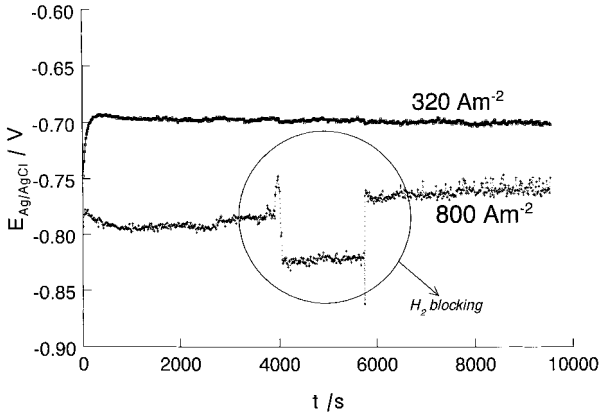

Fig. 4. Potential of RVC-100 as a function of time at 320 and 800 A m^{-2} and under standard conditions.

typical result of the nickel concentration against time dependence is shown in Fig. 5, where it can be seen that the decrease in the nickel concentration is fast in the first hour of electrolysis and slows to practically zero after 4 h. A limiting value of about 2 mM Ni^{2+} is reached.

3.3. *Current efficiency for nickel deposition*

3.3.1. Separator type between cathode and active layer of the gas diffusion anode. Tests were carried out using an E-TEK–GDE combined with a Nafion®-117 membrane, an E-TEK–GDE combined with a perforated Perspex plate or an ECN–GDE without an extra separator, since the latter electrode consisted of a GDE and a Nafion®-117 membrane. The standard bath composition and electrolysis conditions were used. The results of the cell voltage and the nickel current efficiency for the different combinations of electrode and separator are shown in Table 2. Since no nickel hydroxide was deposited on the cathode, it is likely that the decrease in nickel concentration in the solution is caused entirely by metallic nickel deposition.

From these results, it is seen that the type of GDE-separator combination has practically no effect on the current efficiency. The cell voltage was slightly higher when the E-TEK–GDE was used in combination with a Nafion® membrane as compared to the ECN–GDE, but the high cell voltage for a perforated Perspex separator is caused by the large distance, namely 4 mm, between the GDE and the packed bed electrode.

Table 2. Effect of GDE–separator combination

Electrode–separator	*Cell voltage* /V	*Nickel current efficiency* /%
E-TEK–GDE/Nafion®	1.32	34.8
E-TEK–GDE/Perspex	3.85	37
ECN–GDE	0.95	35.6

3.3.2. Type of cathode. Experiments were carried out with an expanded nickel electrode, a RVC-10 electrode and a bed of graphite particles with irregular shapes of which the maximum diameter d_{max} was determined by sieving. The diameter ranges of the graphite particles used were 1 mm < d < 2 mm, 2 mm < d < 4 mm and 4 mm < d < 6 mm. With the exception of the cathode materials, all the other conditions were standard. Nickel current efficiency results for the different cathode types are shown in Fig. 6. From this figure, it is clear that the stack of expanded nickel sheets and the RVC-10 give the highest current efficiencies.

For the graphite bed electrode it was observed that only the graphite particles nearest to the Nafion®-117 membrane had nickel deposits. The depth of the bed with nickel deposition, known as the deposit penetration depth, was observed to be between 2 and 3 mm, depending on the particle size. Moreover, the coarser particles (4 mm < d < 6 mm) gave a larger deposit-penetration depth while the fine particles (1 mm < d < 2 mm) gave a thin layer of metal growth and dendritic growth on and into the Nafion® membrane. With both the expanded nickel sheet and the RVC-10 electrode, the whole electrode depth (8 mm) was covered with nickel deposit, even the graphite current feeder.

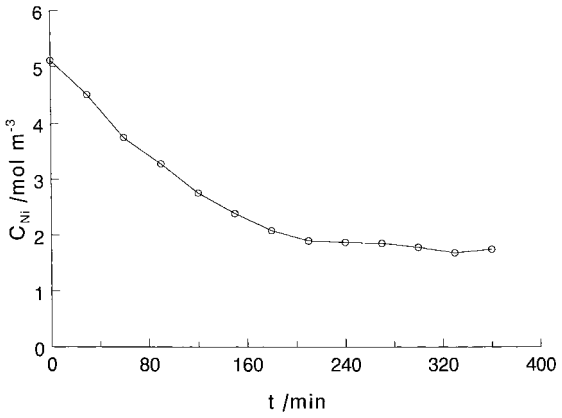

Fig. 5. Nickel concentration against time of electrolysis for a graphite packed bed electrode at 320 A m^{-2}.

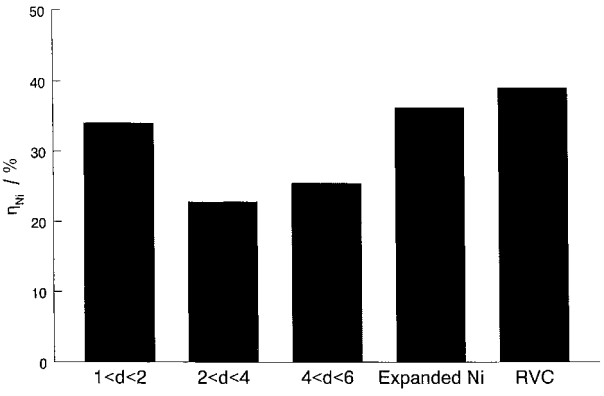

Fig. 6. Effect of graphite particle size and the configuration of the cathode on the nickel current efficiency.

3.3.3. Electrolysis conditions

(a) *Current density*
The current density was varied between 80 and 640 A m^{-2}. All the other standard conditions were maintained. The effect of current density i on current efficiency for the nickel deposition, η_{Ni}, is shown in Fig. 7. The current efficiency increases steadily to a maximum of 28% at $i_{opt} = 380$ A m^{-2}, after which it drops steadily with increasing current density i. At higher currents, deposits were observed to be non-coherent, dark and powdery; probably these deposits were not exclusively metallic nickel but contained some $Ni(OH)_2$. From Fig. 7, it can be deduced that for $i < i_{opt}$, where pure metallic nickel deposit is formed

$$\frac{\eta_{Ni}}{(1-\eta_{Ni})} = 6.77 \times 10^{-3} i^{0.69} \quad (1)$$

and for $i > i_{opt}$, where both metallic nickel and, probably, $Ni(OH)_2$ are deposited

$$\frac{\eta_{Ni}}{(1-\eta_{Ni})} = 48.79 i^{-0.80} \quad (2)$$

(b) *Solution flow rate*
The solution flow rate through the cell was varied between 6 and 21 cm^3 s^{-1}. The effect of the flow rate on nickel current efficiency is shown in Fig. 8. The current efficiency increases steadily but at a decreasing rate as the flow rate increases. It can be deduced that

$$\frac{\eta_{Ni}}{(1-\eta_{Ni})} = 152 Q_l^{0.52} \quad (3)$$

where Q_l is given in m^3 s^{-1}.

(c) *Temperature*
Two temperatures were tested, namely 298 and 328 K, all the other standard conditions being maintained. The results for cell voltage and nickel current efficiency are shown in Table 3. An increase in temperature lowers the cell voltage, while the current efficiency is not significantly affected.

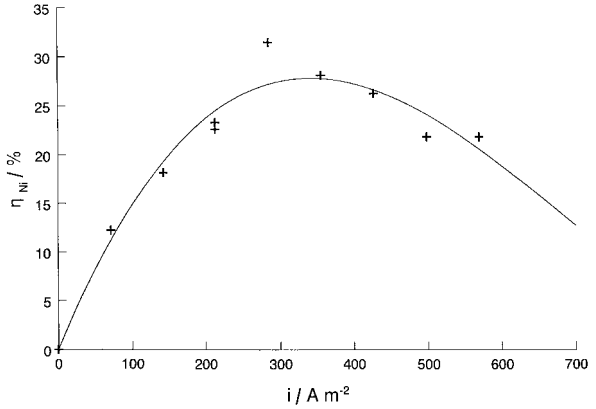

Fig. 7. Effect of the current density on the nickel current efficiency under standard conditions.

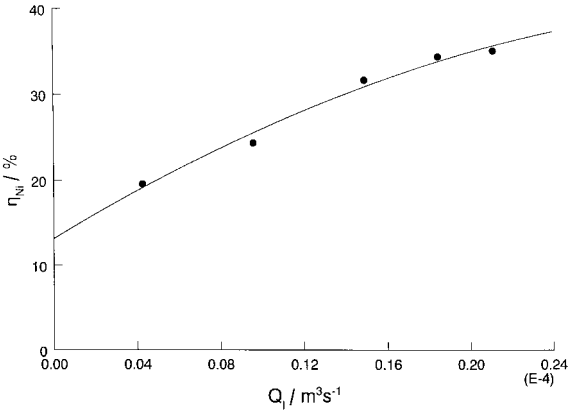

Fig. 8. Effect of the volumetric flow rate density on the nickel current efficiency under standard conditions.

3.3.4. Bath composition

(a) *Boric acid*
The boric acid in the bath was varied between 5 and 180 mol m^{-3}. To exclude the influence of nickel-ammonia complex formation, $(NH_4)_2SO_4$ was not used in these series of experiments. Depositions were carried for 2 h. All other conditions were maintained as in Table 1. The results are shown in Fig. 9. The current efficiency decreases steadily with increasing boric acid concentration from 33.5% at 5 mol m^{-3} to 20% at 180 mol m^{-3}. It can be deduced that for a boric acid concentration above 5 mol m^{-3}, then

$$\frac{\eta_{Ni}}{(1-\eta_{Ni})} = 0.67\ C_{BA}^{-0.19} \quad (4)$$

where C_{BA} is in mol m^{-3}.

(b) *Nickel concentration*
The bath was made up of 0.1 M Na_2SO_4, 20 mM $(NH_4)_2SO_4$ and various initial concentrations of nickel ions between 0.6 and 30 mM. The electrode parameters and electrolysis conditions were kept standard. Nickel current efficiency as a function of initial concentration and average concentration of nickel ions are shown in Fig. 10. It can be seen that for nickel ion concentration below 5 mol m^{-3}, the current efficiency increases rapidly with increasing nickel ion concentration. For concentrations above 5 mol m^{-3}, the increase in current efficiency with increasing concentration is less rapid and almost linear. There is practically no difference between the two curves and neglecting the difference we obtain

$$\frac{\eta_{Ni}}{(1-\eta_{Ni})} = 0.13\ C_{Ni}^{0.67} \quad (5)$$

Table 3. Temperature effect

Temperature /K	*Cell voltage* /V	*Nickel current efficiency* /%
298	0.95	35
328	0.76	37

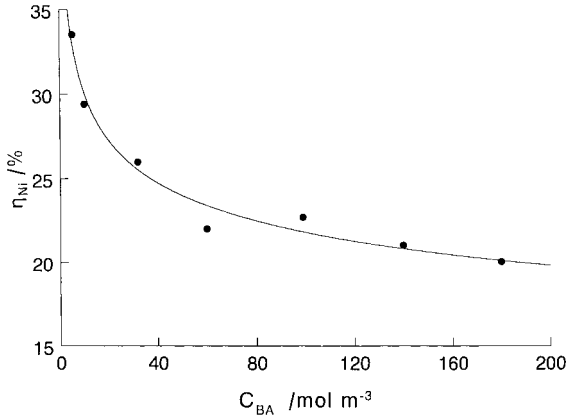

Fig. 9. Effect of boric acid concentration on the nickel current efficiency under standard conditions but without $(NH_4)_2SO_4$.

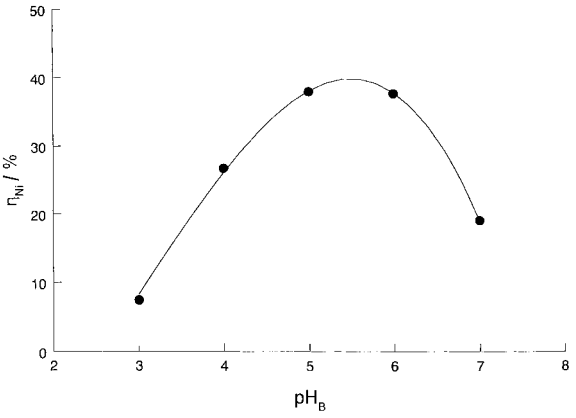

Fig. 11. Effect of bulk solution pH on the nickel current efficiency under standard conditions.

where C_{Ni} is given in mol m^{-3}.

(c) *pH*

The pH of the bath was varied by the addition of NaOH or H_2SO_4 and its initial nickel concentration was 5 mM. The other conditions were standard. The results are shown in Fig. 11. The current efficiency goes through a maximum of 40% at pH of 5.5, and two distinct pH regions can be described. For pH < 5.5 where only metallic nickel is formed

$$\frac{\eta_{Ni}}{(1-\eta_{Ni})} = 0.3\ \mathrm{pH} - 0.71 \qquad (6)$$

and for pH > 5.5 where both metallic nickel and probably $Ni(OH)_2$ are deposited

$$\frac{\eta_{Ni}}{(1-\eta_{Ni})} = -0.4\ \mathrm{pH} + 2.8 \qquad (7)$$

4. Discussion

4.1. *Electrode configuration*

From Section 3.3.1 and Table 2 it follows that the current efficiency for nickel deposition is not affected by the type of GDE and the nature of separator between the active layer of the GDE and the three-dimensional cathode. This means that the cathodic process can be considered separately. Figure 5 shows that the configuration of the three-dimensional cathode affects the nickel current efficiency as well as the deposit penetration depth. The bed with the smallest graphite particles, the RVC-100 and the expanded metal electrode give practically equal current efficiencies being significantly higher than those for beds with bigger graphite particles.

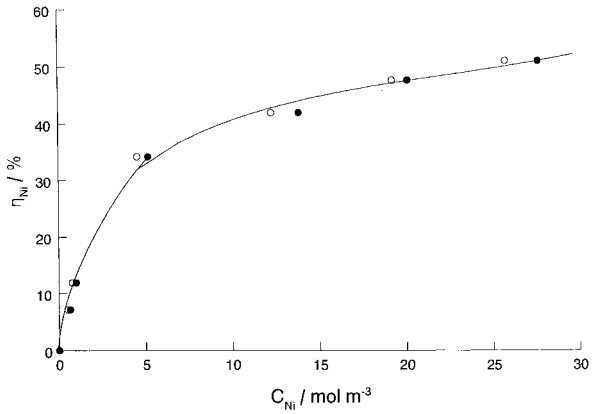

Fig. 10. Effect of initial (•) and average (○) nickel concentration on the nickel current efficiency. The bath consisted of 0.1 M Na_2SO_4, 20 mM $(NH_4)_2SO_4$ and various concentrations of nickel ions.

Because of the low porosity of the graphite particles, hydrogen gas bubbles formed during electrolysis can stick very easily in the void spaces between the graphite particles in the packed bed. An accumulation of gas bubbles within the bed hinders the current through the electrolyte and diminishes the penetration depth of the current. Despite the high porosity of RVC-100 (~0.91), cathode potential jumps of about 60 mV were observed at a high apparent current density, namely 800 A m^{-2}, due to partial blockage of the RVC electrode by hydrogen gas bubbles (Fig. 4). The gas bubbles accumulate within the pores leading to a significant decrease in pore electrolyte conductivity [9]. This effect was not found for the expanded metal electrode. Expanded metal electrodes have been reported to be very effective in diverting gas bubbles, resulting in a significant decrease in ohmic drop and cell voltage [10].

For long-term use, the nickel deposit will block the small pores within the RVC-100 and the bed of graphite particles, in particular, the pores lying near the gas diffusion anode. This means that only a small part of the bed is then used for nickel deposition. This is confirmed by the distribution of the nickel over the thickness of the RVC-100 material and the packed bed (Section 3.3.2). Since the voids within the stack of expanded metal are much bigger than those of a packed bed of graphite particles, the deposit-penetration depth is much larger for the former than for the latter. Despite the RVC-10 and RVC-100 having nearly the same porosity (0.97 and 0.91, respectively), the penetration depth for nickel deposition was much smaller for the latter than for the former. The main difference between the two RVC materials is the pore size and, thus, the specific surface area. In practice, a stack of expanded metal sheets is a useful electrode

for metal deposition when the metal deposit is re-used as an anode material.

4.2. *Electrolysis conditions and bath composition*

The current efficiency of nickel deposition depends on many parameters: it increases with increasing current density up to a fixed value (Fig. 7 and Section 3.3.3(a)), increasing volumetric flow rate of solution (Fig. 8), increasing nickel concentration (Fig. 10), decreasing boric acid concentration (Fig. 9) and increasing pH up to a fixed value. Temperature has practically no effect upon the current efficiency for nickel deposition. Electrochemical deposition of nickel is accompanied by hydrogen evolution, leading to elevated pH values on the cathode surface.

The pH of the solution at the electrode surface is very important and determines the nature of the deposit on the electrode; at a high pH (e.g., >5.5) $Ni(OH)_2$ precipitation takes place on the electrode surface, and this precipitate covers the cathode surface and inhibits the reduction of metal ions to metallic nickel. The pH of the solution at the cathode surface also depends on many parameters. Hessami *et al.* [11] have reported that the formation of metal hydroxide is due to a high surface pH and depends on mass transfer conditions, current density, solution chemistry determined by pH of the bulk solution, buffering agents and nickel concentration.

Ji *et al.* [12] have suggested three factors which can suppress the increase in the surface pH of the cathode. The first is the mass transfer of hydrogen ions towards the surface, the second is the proton-donating pH buffers, such as boric acid or bisulfate ions and the third factor is the hydroxyl-consuming agent, such as $NiOH^+$ and $Ni_4(OH)_4^{4+}$.

Three pH ranges can be distinguished, namely bulk solution pH $<$ 5 with only metallic nickel deposition and bulk solution pH $>$ 9 with only green nickel hydroxide precipitation and the transition range between bulk solution pH 5 and 9 where both compounds are formed [7]. Three similar pH ranges can also be seen in Fig. 11, where the current efficiency is given as a function of bulk solution pH.

The nickel deposition is first discussed for the experimental conditions where metallic nickel deposit is exclusively formed, namely $i < 380\,A\,m^{-2}$, as given in Fig. 7 and at pH $<$ 5.5 as given in Fig. 11. Metallic nickel deposit is also obtained under the experimental conditions for Fig. 9 and Fig. 10. Results shown on Fig. 10 are comparable to the results reported for reduction of nickel ions in a Chemelec Cell [14]. From these figures, it has been deduced that for a metallic Ni deposit $\eta_{Ni}/(1-\eta_{Ni})$ is proportional to $i^{0.69}, Q_1^{0.52}$, $C_{Ni}^{0.67}, C_{BA}^{-0.19}$ and $pH^{1.0}$

In [13], similar linear equations have been derived to relate the current efficiency for a metal to the current density, temperature, pH and concentration of metal ions reduced at the cathode, where the current efficiency is only determined by the kinetic parameters of the metal deposition and hydrogen evolution and the concentration of metal and hydrogen ions. It can also be shown from the results of rotating disc electrode (RDE) experiments presented in [7] that $\eta_{Ni}/(1-\eta_{Ni})$ is proportional to $i^{1.0}$, $\omega^{0.16}$, $C_{AM}^{-0.19}$ and $pH^{1.0}$, where ω is the rotational speed and C_{AM} is the concentration of NH_4OH. Comparing the results of a RDE to the results of a packed bed electrode (PBE) above, it is seen that two distinct types of parameters may be identified namely those parameters with a global effect and parameters with a local effect. The pH and concentration of the complexing agent have been identified as global parameters, their effects being independent of the electrode configuration. The current density, nickel ion concentration and the solution convection however have been identified as local parameters in the sense that their effect depends on the electrode configuration and therefore on the location within the packed bed electrode. This is because the effect of these parameters on a particular location depends on the potential and current density distribution within the PBE. The proportionalities on these parameters reported above represent the effects averaged over the whole bed. Any change in the bed parameters that affects the potential and current density distribution is bound to affect these proportionalities. To describe the reduction of Ni^{2+} at the packed bed electrode adequately it is necessary to set up a set of relations describing the current density and potential distribution over the packed bed electrode.

In [7], the rate of metallic nickel deposition was determined as a function of pH on a rotating disc electrode and a similar η_{Ni}–pH curve was found, as shown in Fig. 11. It is likely that at pH $>$ 5.5, the ratio between metallic nickel and nickel hydroxide deposition decreases with increasing pH. It is well known that the $NiOH^+$ ion is formed in nickel solutions with a pH $>$ 5[15]. When the supply of hydrogen ions is unable to meet the depletion rate, the cathode surface pH will rise and eventually lead to the formation of insoluble nickel hydroxide on the cathode surface. Moreover, in the presence of boric acid, nickel boric acid complexes such as $Ni(H_2BO_3)_2$ and possibly $Ni(H_2BO_3)^+$, are formed. These complexes will diminish the overall reaction rate constant of metallic nickel deposition. Dissociation of boric acid produces H^+ ions and enhances the rate of hydrogen evolution. Consequently, the decrease in η_{Ni} with increasing boric acid concentration can be explained. Boric acid buffers nickel electrolytes in the pH region 5.5–6.5, depending on the Ni^{2+} content in the solution [16]. In the absence of boric acid, the surface pH may rise above the limit where precipitation of $Ni(OH)_2$ occurs. The presence of boric acid depresses the surface pH, around the buffer pH, where deposition of nickel is possible, for a wider range of bulk solution pH. The use of buffering agents during electrochemical deposition of nickel from dilute baths is necessary [7]. It has been reported that boric acid also acts as a catalyst to reduce the over-voltage for nickel deposition [17]. However,

when working with low nickel concentrations the optimum concentration of boric acid becomes critical. With a nickel concentration of $5\,mol\,m^{-3}$, the optimum concentration of boric acid is less than $5\,mol\,m^{-3}$.

Nickel ions are removed from the solution by precipitation of $Ni(OH)_2$ on the cathode at pH > 9, where no metallic nickel is formed and the electric charge is completely used for hydrogen evolution. Due to this hydrogen formation, the pH at the cathode surface becomes much higher than the pH of the bulk solution, resulting in $Ni(OH)_2$ precipitation.

References

[1] D. Genders and N. Weinberg, 'Electrochemistry for a Cleaner Environment', The Electrosynthesis Company (1992)
[2] J. H. Clark, 'Chemistry of Waste Minimization', 1st edn, Blackie Academic & Professional, New York (1995).
[3] R. Suzuki, W-H Li, M. Schwartz and K. Nobe, *Plat. Surf. Finish.* Dec. (1995) 58.
[4] Supplier's documents from ElectroCell AB, Sweden.
[5] L. J. J. Janssen, Dutch Patent *9 101 022* (1991).
[6] E. C. W Wijnbelt and L. J. J. Janssen, *J. Appl. Electrochem.* **24** (1994) 1028.
[7] K. N. Njau and L. J. J. Janssen, *ibid.* **25** (1995) 982.
[8] K. N. Njau, W.-J. Van Der Knaap and L. J. J. Janssen, *J. Appl. Electrochem.* **28** (1998) 343.
[9] M. M. Saleh and J. W. Weidner, *J. Electrochem. Soc.* **142** (1995) 4113.
[10] S. Piovano, O. N. Cavatorta and U. Bohm, *J. Appl. Electrochem.* **18** (1988) 128.
[11] S. Hessami and C. Tobias, *J. Electrochem. Soc.* **136** (1989) 3611.
[12] J. Ji, W. C. Cooper, D. B. Dreisinger and Peters, *J. Appl. Electrochem.* **25** (1995) 642.
[13] P. Yu and R. Perelygin, *J. Electrochem.* **30** (1994) 10.
[14] W. C. Grande and J. B. Talbot, *J. Electrochem. Soc.* **140** (1993) 675.
[15] D. A. Campbell, I. M. Dalrymple, J. G. Sunderland and D. Tilston, *Resources Conservation and Recycling* **10** (1994) 25.
[16] B. V. Tilak, A. S. Gendron and M. A. Mosoiu, *J. Appl. Electrochem.* **7** (1977) 495.
[17] D. Gangasingh and J. B. Talbot, *J. Electrochem. Soc.* **138** (1991) 3605.